Temperature dependence and aging effects on silicon nanowires photoluminescence

Pietro Artoni,[1,2] Alessia Irrera,[3] Fabio Iacona,[1,*] Emanuele F. Pecora,[1,2] Giorgia Franzò,[1] and Francesco Priolo[1,2]

[1]*MATIS IMM-CNR, via S. Sofia, 64, 95123 Catania, Italy*
[2]*Dipartimento di Fisica e Astronomia, Università di Catania, via S. Sofia, 64, 95123 Catania, Italy*
[3]*IPCF-CNR, viale F. Stagno d'Alcontres 37, Faro Superiore, 98158 Messina, Italy*
[*]*fabio.iacona@ct.infn.it*

Abstract: In this paper we describe the luminescence properties of Si nanowires (NWs) prepared by a maskless synthesis technique, based on the Au-catalyzed wet etching of Si substrates by an aqueous solution of H_2O_2 and HF. A strong room temperature photoluminescence (PL), centered at about 690 nm, is observed when Si NWs are optically excited. The detailed analysis of the steady-state and time-resolved PL properties of the system as a function of aging, temperature and pump power allows to demonstrate that the emission is due to the radiative recombination of quantum confined excitons. These results open the route towards novel applications of Si NWs in photonics as efficient light sources.

OCIS codes: (160.4236) Nanomaterials; (250.5230) Photoluminescence; (350.3850) Materials processing; (160.6000) Semiconductor materials; (350.4238) Nanophotonics and photonic crystals.

References and links

1. U. Gösele, "How clean is too clean?" Nature **440**(7080), 34–35 (2006).
2. B. Tian, X. Zheng, T. J. Kempa, Y. Fang, N. Yu, G. Yu, J. Huang, and C. M. Lieber, "Coaxial silicon nanowires as solar cells and nanoelectronic power sources," Nature **449**(7164), 885–889 (2007).
3. X. T. Zhou, J. Q. Hu, C. P. Li, D. D. D. Ma, C. S. Lee, and S. T. Lee, "Silicon nanowires as chemical sensors," Chem. Phys. Lett. **369**(1–2), 220–224 (2003).
4. L. Pavesi and R. Turan, *Silicon Nanocrystals. Fundamentals, Synthesis and Applications* (Wiley-VCH, Weinheim, 2010).
5. R. S. Wagner and W. C. Ellis, "Vapor-liquid-solid mechanism of single crystal growth," Appl. Phys. Lett. **4**(5), 89–90 (1964).
6. B. J. Kim, J. Tersoff, S. Kodambaka, M. C. Reuter, E. A. Stach, and F. M. Ross, "Kinetics of individual nucleation events observed in nanoscale vapor-liquid-solid growth," Science **322**(5904), 1070–1073 (2008).
7. V. Schmidt, S. Senz, and U. Gösele, "Diameter-dependent growth direction of epitaxial silicon nanowires," Nano Lett. **5**(5), 931–935 (2005).
8. M. Shao, L. Cheng, M. Zhang, D. D. D. Ma, J. A. Zapien, S.-T. Lee, and X. Zhang, "Nitrogen-doped silicon nanowires: synthesis and their blue cathodoluminescence and photoluminescence," Appl. Phys. Lett. **95**(14), 143110 (2009).
9. O. Demichel, V. Calvo, N. Pauc, A. Besson, P. Noé, F. Oehler, P. Gentile, and N. Magnea, "Recombination dynamics of spatially confined electron-hole system in luminescent gold catalyzed silicon nanowires," Nano Lett. **9**(7), 2575–2578 (2009).
10. S. S. Walavalkar, C. E. Hofmann, A. P. Homyk, M. D. Henry, H. A. Atwater, and A. Scherer, "Tunable visible and near-IR emission from sub-10 nm etched single-crystal Si nanopillars," Nano Lett. **10**(11), 4423–4428 (2010).
11. J. Valenta, B. Bruhn, and J. Linnros, "Coexistence of 1D and quasi-0D photoluminescence from single silicon nanowires," Nano Lett. **11**(7), 3003–3009 (2011).
12. A. R. Guichard, D. N. Barsic, S. Sharma, T. I. Kamins, and M. L. Brongersma, "Tunable light emission from quantum-confined excitons in $TiSi_2$-catalyzed silicon nanowires," Nano Lett. **6**(9), 2140–2144 (2006).
13. K. Q. Peng, Y. Wu, H. Fang, X. Y. Zhong, Y. Xu, and J. Zhu, "Uniform, axial-orientation alignment of one-dimensional single-crystal silicon nanostructure arrays," Angew. Chem. Int. Ed. Engl. **44**(18), 2737–2742 (2005).
14. Z. Huang, T. Shimizu, S. Senz, Z. Zhang, N. Geyer, and U. Gösele, "Oxidation rate effect on the direction of metal-assisted chemical and electrochemical etching of silicon," J. Phys. Chem. C **114**(24), 10683–10690 (2010).
15. K. Q. Peng, Y. Xu, Y. Wu, Y. J. Yan, S. T. Lee, and J. Zhu, "Aligned single-crystalline Si nanowire arrays for photovoltaic applications," Small **1**(11), 1062–1067 (2005).

#157097 - $15.00 USD Received 25 Oct 2011; revised 7 Dec 2011; accepted 7 Dec 2011; published 9 Jan 2012

16. V. A. Sivakov, F. Voigt, A. Berger, G. Bauer, and S. H. Christiansen, "Roughness of silicon nanowire sidewalls and room temperature photoluminescence," Phys. Rev. B **82**(12), 125446 (2010).
17. S. L. Cheng, C. H. Chung, and Y. H. Chang, "Formation kinetics and structures of high-density vertical Si nanowires on (111)Si substrates," J. Ceram. Process. Res. **10**(3), 243–247 (2009).
18. Z. Huang, T. Shimizu, S. Senz, Z. Zhang, X. Zhang, W. Lee, N. Geyer, and U. Gösele, "Ordered arrays of vertically aligned [110] silicon nanowires by suppressing the crystallographically preferred <100> etching directions," Nano Lett. **9**(7), 2519–2525 (2009).
19. H. Fang, Y. Wu, J. Zhao, and J. Zhu, "Silver catalysis in the fabrication of silicon nanowire arrays," Nanotechnology **17**(15), 3768–3774 (2006).
20. A. Irrera, P. Artoni, R. Saija, P. G. Gucciardi, M. A. Iatì, F. Borghese, P. Denti, F. Iacona, F. Priolo, and O. M. Maragò, "Size-scaling in optical trapping of silicon nanowires," Nano Lett. **11**(11), 4879–4884 (2011).
21. A. C. Dillon, P. Gupta, M. B. Robinson, A. S. Bracker, and S. M. George, "FTIR studies of water and ammonia decomposition on silicon surfaces," J. Electron Spectrosc. Relat. Phenom. **54-55**, 1085–1095 (1990).
22. M. S. Brandt, H. D. Fuchs, M. Stutzmann, J. Weber, and M. Cardona, "The origin of visible luminescence from 'porous silicon': a new interpretation," Solid State Commun. **81**(4), 307–312 (1992).
23. M. L. Brongersma, P. G. Kik, A. Polman, K. S. Min, and H. A. Atwater, "Size-dependent electron-hole exchange interaction in Si nanocrystals," Appl. Phys. Lett. **76**(3), 351–353 (2000).
24. P. D. J. Calcott, K. J. Nash, L. T. Canham, M. J. Kane, and D. Brumhead, "Identification of radiative transitions in highly porous silicon," J. Phys. Condens. Matter **5**(7), L91–L98 (1993).
25. V. Vinciguerra, G. Franzò, F. Priolo, F. Iacona, and C. Spinella, "Quantum confinement and recombination dynamics in silicon nanocrystals embedded in Si/SiO_2 superlattices," J. Appl. Phys. **87**(11), 8165–8173 (2000).
26. M. Palummo, F. Iori, R. Del Sole, and S. Ossicini, "Giant excitonic exchange splitting in Si nanowires: First-principles calculations," Phys. Rev. B **81**(12), 121303 (2010).
27. G. Franzò, A. Irrera, E. C. Moreira, M. Miritello, F. Iacona, D. Sanfilippo, G. Di Stefano, P. G. Fallica, and F. Priolo, "Electroluminescence of silicon nanocrystals in MOS structures," Appl. Phys., A Mater. Sci. Process. **74**(1), 1–5 (2002).

1. Introduction

Silicon nanowires (NWs) represent a very promising system to become the building blocks for future electronic devices [1], photovoltaic cells [2], and sensors [3]. On the other hand, while the search for innovative strategies to make silicon an efficient light emitter at room temperature is extremely active [4], light emission from Si NWs is still a quite rarely observed, and often not fully understood, phenomenon. The main reason for this seeming lack of interest is that, while it is well known that carrier quantum confinement is the mechanism ruling the efficient room temperature emission from Si nanocrystals (nc) [4] or porous Si [4], all the main techniques used for Si NWs synthesis, including those based on the vapor-liquid-solid (VLS) mechanism and those exploiting top-down lithographic processes, can very hardly produce NWs having a size compatible with the occurrence of quantum confinement effects [5–7]. A further problem related with the VLS growth is the incorporation of the metal catalyst in the NWs; indeed Au, the most used catalyst, acts as a deep non-radiative recombination center, thus negatively altering both electronic and optical properties. In agreement with the above considerations, photoluminescence (PL) emission from Si NWs has been attributed to the presence of N-containing complexes [8] or to the phonon-assisted low temperature recombination of photogenerated carriers [9]. PL emission from Si NWs due to quantum confinement has been only obtained by reducing, through thermal oxidation processes, the diameter of NWs obtained by plasma etching of a Si wafer [10,11], or by a $TiSi_2$-catalyzed VLS growth [12]; however, the oxidation approach constitutes a serious obstacle if NW applications involving electrical conduction (such as the fabrication of light emitting devices) are sought for.

Having as the main goal the fabrication of NWs with an extremely small diameter, such as to lead to the observation of quantum confinement effects, it is clear that, in general, VLS-based techniques are not suitable for this purpose, since the well known Gibbs-Thomson effect limits the minimum obtainable radius. On the other hand, the top-down approach requires expensive and time-consuming lithographic processes (typically electron-beam lithography) to produce sizes which are close to those required for an efficient carrier confinement. Within this context, metal-assisted wet etching processes, which usually employ as a catalyst a metal salt (typically $AgNO_3$) [13–16], may constitute an interesting alternative, since they are direct etching processes, which do not need any kind of complex lithographic procedure. However this technique, although very widely used for NW synthesis, is not able

#157097 - $15.00 USD Received 25 Oct 2011; revised 7 Dec 2011; accepted 7 Dec 2011; published 9 Jan 2012

to control the NW size in the few-nm range; furthermore, the process, although not involving metal inclusion in the NW, leads to the formation of dendrites, whose subsequent removal could damage the NWs [13,17].

The development of metal assisted wet etching processes in which the salt is replaced by a metal (Au or Ag) ultra-thin film deposited on the substrate surface [18–20] allows to simultaneously avoid dendrite formation and metal inclusion inside the NWs. By using this technique residual metal particles are indeed trapped at the bottom of the etched regions, and they can be effectively removed by a suitable selective etching process, without contaminating the NWs. Furthermore, this modification makes the process simple, cheap, fast and compatible with Si technology and, more importantly, it allows a greater control over the Si NWs structural properties (and above all, over the diameter).

In this paper, we report and discuss the detailed analysis of the steady-state and time-resolved PL properties of very dense (about 1×10^{11} cm^{-2}) arrays of long (2.6 μm) and small (diameter of 7 ± 2 nm) Si NWs as a function of aging, pump power and temperature. The presented optical data constitute convincing evidences that the emission from Si NWs is due to the occurrence of quantum confinement effects and give important insights about the nature of the exciton recombination processes. The possibility to obtain an efficient room temperature light emission from Si NWs represents a great advancement and opens the way to a wide range of new and unexpected photonic applications for this material.

2. Experimental section

Si NWs have been obtained starting from p-type (B concentration of 10^{16} cm^{-3}) single crystal, (100)-oriented Si wafers. The wafers were cut into 1 cm × 0.3 cm pieces, and then UV oxidized and dipped in 5% HF to obtain clean and oxide-free Si surfaces. Afterwards, a thin Au layer (about 2 nm) was deposited on the Si samples at room temperature by electron beam evaporation by using high purity (99.9%) Au pellets as a source. Finally, samples were etched at room temperature in an aqueous solution of HF (5 M) and H_2O_2 (0.44 M) for 600 s to form Si NWs.

NW structural characterization was performed by scanning electron microscopy (SEM); plan view and cross section SEM analyses were performed by a field emission Zeiss Supra 25 microscope. PL measurements were performed by pumping with the 488 nm line of an Ar^+ laser. The laser beam was chopped by an acousto-optic modulator at a frequency of 55 Hz. PL signals were analyzed by a single-grating monochromator and detected by a water cooled photomultiplier tube. Time resolved PL measurements were performed by monitoring the decay of the PL signal at 690 nm after pumping to steady state and switching off the laser beam. The overall time resolution of our system is 30 ns. Low temperature measurements were performed by using a closed cycle He cryostat with the samples kept in vacuum at a pressure of 10^{-5} Torr.

3. Results and discussion

Figure 1 reports a cross section SEM image of Si NWs obtained by the metal-assisted wet etching technique. The image displays a dense and uniform distribution of NWs, having the same length of about 2.6 μm and a mean diameter of 7 ± 2 nm, as determined by Raman measurements. The analysis of plan view SEM images allows to estimate a very high NW density of 1×10^{11} cm^{-2}. The very large aspect ratio and the very high density of the NWs are highly remarkable and can be hardly obtained by techniques based on the VLS mechanism [6, 7].

The Si NWs are efficient light emitters at room temperature. The inset of Fig. 2 reports a typical PL spectrum obtained by exciting the sample with the 488 line of an Ar^+ laser at a pump power of 10 mW. The spectrum consists of a broad band (full width at half maximum of about 150 nm) centered at ~690 nm. It is interesting to note that the PL spectrum reported in the inset has been measured after about 150 days from NW synthesis; we noticed indeed

#157097 - $15.00 USD Received 25 Oct 2011; revised 7 Dec 2011; accepted 7 Dec 2011; published 9 Jan 2012

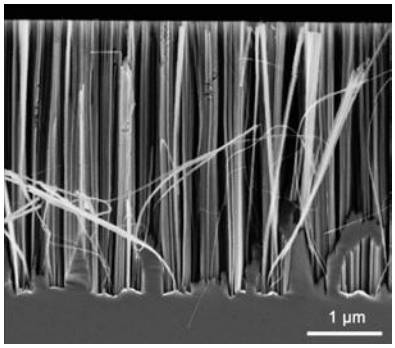

Fig. 1. Cross section SEM image of Si NWs obtained by metal-assisted wet etching of a Si substrate.

that the PL signal of this material exhibits a marked aging effect. This behavior is illustrated in Fig. 2, where the intensity of the PL signal at 690 nm of freshly prepared Si NWs is plotted as a function of the air exposure time, at room temperature.

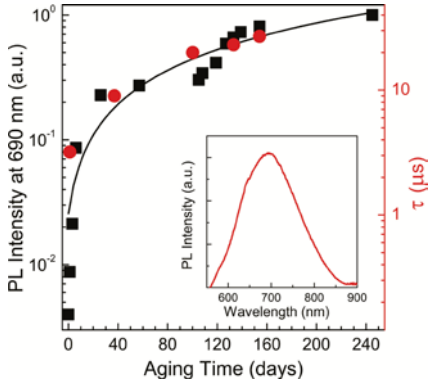

Fig. 2. Normalized intensity of the PL signal at 690 nm of freshly prepared Si NWs as a function of the air exposure time at room temperature (black squares). The line is a linear fit to the data. The lifetime of the PL signal, obtained by following the decrease of the PL signal at 690 nm after the laser switch-off, as a function of the aging is also presented (red circles, right-hand scale). During the experiment the sample is exposed to the laser beam only for the brief time needed for PL data acquisition. The inset reports a typical PL spectrum obtained from a 150-days-aged sample. The PL data are obtained by exciting the sample with the 488 nm line of an Ar^+ laser at a pump power of 10 mW.

The PL signal is seen to monotonically increase as a function of the air exposure time; the experiment has been conducted up to 245 days, and within this time lapse, an increase of the PL intensity accounting for a factor of 250 has been found. No noticeable variation of the peak position and shape has been observed during the whole experiment.

Two different interpretations of the observed aging phenomenon are possible: since it is known that Si surfaces, especially if freshly etched, can interact with atmospheric reactive gases such as O_2 or H_2O [21], the increase of the PL signal as a function of air exposure time can be due to the formation of new luminescent surface states. Under this hypothesis, the PL from Si NWs should be due to surface emitting centers (such as siloxene and its derivates [22]) whose number increases due to the progress of the surface reactions with gaseous species. In contrast, since it is well known that Si nanostructures exhibiting quantum confinement effects need an efficient surface passivation in order to suppress the non radiative de-excitation channels which could limit the efficiency of the light emission process, the effect of aging could be ascribed to an improvement of the surface passivation of the quantum confined Si NWs, through heterogeneous (gas-solid) reactions involving O_2 or H_2O, leading to the formation of Si-H, Si-O or Si-OH bonds.

#157097 - $15.00 USD Received 25 Oct 2011; revised 7 Dec 2011; accepted 7 Dec 2011; published 9 Jan 2012

To discriminate between the two above described effects, we have studied the lifetime of the PL signal as a function of the aging by following the decrease of the PL signal at 690 nm after the laser switch-off. The lifetime data are reported in Fig. 2 as red points and indicate the occurrence of an increase of the lifetime as a function of the aging; in particular, a lifetime value of about 30 μs has been observed in 245-days-aged samples. This value is about two orders of magnitude longer than that reported for Si pillars produced by e-beam lithography and subsequently thinned by thermal oxidation [10]. The common trend as a function of the aging exhibited by PL intensity and lifetime strongly suggests that aging produces an efficient surface passivation of the quantum confined NWs, and, in turn, a reduction of the number of sites acting as centers for non-radiative recombination. The occurrence of quantum confinement effects has been confirmed by the observation that the PL signal can be shifted by synthesizing NWs having a different mean size. We remark finally that the absence of saturation of the PL intensity in the explored time range (the behavior is roughly linear within the whole time lapse) puts clearly into evidence the huge surface area of this material.

The effect of passivation on the PL properties of Si NWs has been also studied by following the behavior of the PL intensity at 690 nm during a prolonged exposure to the laser source used for PL experiments (488 nm, 10 mW). The results are reported in Fig. 3; in particular, the red points illustrate the behavior of the PL intensity at 690 nm of 150 days-aged Si NWs when the laser is left on the sample kept in air. The PL intensity increases by approximately a factor of 1.5 in a time lapse of 2000 s; the increase of the signal is sub-linear but, remarkably, no steady state is reached even in longer experiments.

The effect of the laser resembles that of an accelerated aging; indeed the laser-induced decomposition of gaseous molecules such as O_2 or H_2O increase the rate of the heterogeneous surface reactions leading to the NW passivation. Since also laser-induced desorption phenomena simultaneously occur, the observed increase of the PL signal is the result of the competition between the two effects. This explains the sublinear increase of the PL intensity shown in Fig. 3, to be compared with the linear increase of Fig. 2, where no phenomena competing with passivation are operating. On the other hand, if, after the 2000 s laser exposure, the sample is transferred in vacuum at a pressure of about 10^{-5} Torr, and we continue the laser exposure, the PL signal at 690 nm is seen to progressively decrease (blue points in Fig. 3), and an intensity lower than the initial one (represented by the dashed line) is reached in a few thousands of seconds. This effect is due to the fact that, in vacuum, no further formation of surface oxidized species can occur and desorption becomes the only operating phenomenon. As a final result, the PL intensity decreases because, in absence of a good surface passivation, non-radiative processes limit the PL efficiency of the system. It is

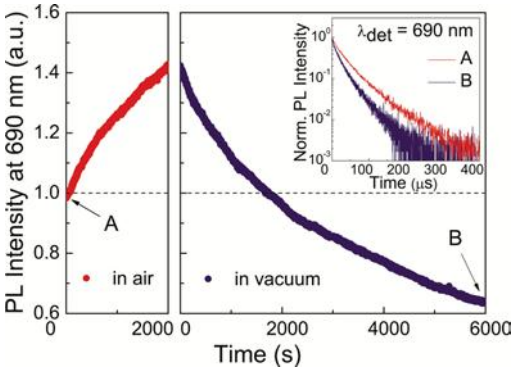

Fig. 3. Normalized intensity of the PL signal at 690 nm of 150 days-aged Si NWs as a function of the exposure time to an Ar^+ laser beam (488 nm, 10 mW). Data refer to laser irradiation with the sample kept in air (red points) or in vacuum (blue points). The dashed line represents the starting PL intensity. In the inset, the comparison between the PL decay curves of 150-days-aged NWs, at the beginning of the irradiation experiment (indicated with A) and after irradiation in vacuum for 6000 s (indicated with B), is reported.

#157097 - $15.00 USD Received 25 Oct 2011; revised 7 Dec 2011; accepted 7 Dec 2011; published 9 Jan 2012

remarkable that the PL intensity observed at the end of the experiment is weaker than the starting one, since this demonstrates that laser irradiation in vacuum is able not only to destroy the effect of the laser irradiation in air, but also to partially remove the NW passivation due to the 150 days of aging of the sample.

We underline that the experiments illustrated in Fig. 3 have been conducted by recording the whole PL spectrum. No relevant variations of the shape (including both the FWHM and the position of the maximum) of the PL peaks were found during the whole experiment, so that the conclusions derived from the figure do not change if we replace the PL intensity at a single wavelength with the integrated PL intensity. The inset of Fig. 3 reports the comparison between the PL decay curves at 690 nm of 150-days-aged NWs, at the beginning of the irradiation experiment (indicated by A) and after irradiation in vacuum for 6000 s (indicated by B). The above discussed enhanced efficiency of non-radiative processes in samples irradiated in vacuum is clearly evidenced by the lifetime shortening from 27 to 16 μs.

The PL properties of the system have been also analyzed as a function of the flux of 488 nm photons. Data are presented in Fig. 4(a); the integrated PL intensity of 150 days-aged Si NWs increases linearly by increasing the photon flux up to a value of 6.2×10^{20} $cm^{-2}s^{-1}$, while at higher fluxes a marked tendency to saturation is seen.

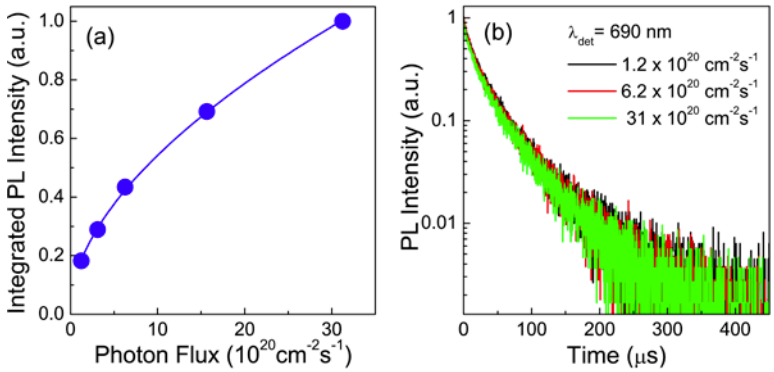

Fig. 4. PL properties of 150 days-aged Si NWs as a function of the flux of 488 nm photons. (a) Normalized integrated PL intensity. The line is a guide to the eyes. (b) Time decay curves of the PL signal measured at 690 nm.

To better understand the above behavior, we have measured the lifetime of the PL signal at 690 nm at different photon fluxes; some selected PL decay curves are reported in Fig. 4(b) and clearly demonstrate that, in the explored range, no appreciable lifetime variation occurs, being the same value of about 20 μs found for all the studied fluxes. This behavior suggests that Auger non-radiative recombination processes do not play a relevant role in competition with the photon emission process.

The experiments described above, and particularly the aging experiment, constitute a valuable help for assigning the PL from Si NWs to the radiative recombination of quantum confined excitons. Further information about the origin of the PL from Si NWs, as well as useful information about their perspectives for practical applications, can be obtained by following the temperature dependence of the PL signal. These measurements are reported in Fig. 5(a), where the PL intensity (IPL) at 690 nm of 150 days-aged Si NWs is plotted as a function of the temperature in the range 11-300 K.

The data show that I_{PL} monotonically increases with the temperature up to about 270 K, where the maximum intensity is found. Above this temperature a slight decrease of I_{PL} is observed. The overall dependence on temperature is relatively weak, since the intensity change between 11 and 270 K accounts for about one order of magnitude.

The PL lifetime as a function of the temperature, measured at a fixed wavelength of 690 nm is reported in Fig. 5(b). The figure shows that the PL lifetime decreases by increasing the

#157097 - $15.00 USD Received 25 Oct 2011; revised 7 Dec 2011; accepted 7 Dec 2011; published 9 Jan 2012

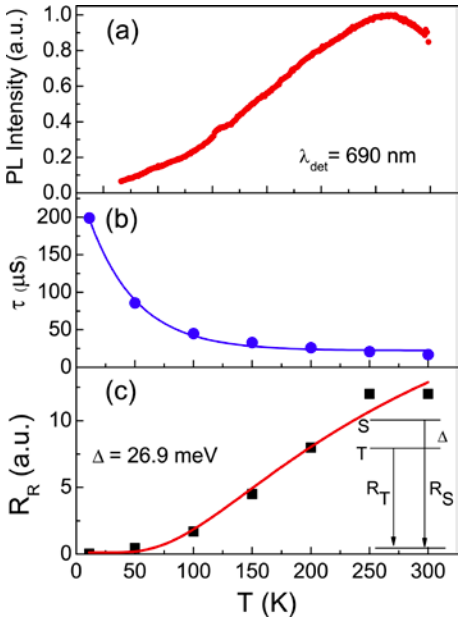

Fig. 5. PL properties of 150 days-aged Si NWs as a function of the temperature in the range 11-300 K. (a) Normalized intensity of the PL signal at 690 nm. (b) Lifetime of the PL signal, measured at a fixed wavelength of 690 nm. The blue line is a guide to the eyes. (c) Radiative rate ($R_R = 1/\tau_{rad}$), extracted by the ratio between the PL intensity and the decay time at a fixed photon flux. The red line is a fit to the data, according to the model proposed in Refs. 23-25, with $\Delta = 26.9 \pm 4.3$ meV. In the inset the singlet and triplet energy levels split by the electron-hole exchange energy Δ are schematically shown.

temperature; in particular, the decay time decreases from 200 μs at 11 K to 20 μs at room temperature, with a variation of about one order of magnitude. This behavior closely resembles that of quantum confined Si systems, such as Si nc [23] and porous Si [24], and it is a further confirmation of the occurrence of quantum confinement effects in Si NWs.

It has been previously demonstrated [25] that, by solving the appropriate rate equation, the PL intensity I_{PL} can be expressed as shown in Eq. (1):

$$I_{PL} \propto \sigma\varphi\frac{\tau}{\tau_{rad}}N \qquad (1)$$

where σ is the excitation cross section, φ the pumping beam photon flux, N the total population of emitting centers, τ the luminescence decay time, including both radiative and non-radiative processes and τ_{rad} the radiative lifetime.

In the low pump power regime, I_{PL} increases linearly with pump power and it is proportional to the ratio τ/τ_{rad}. Since N and σ are temperature independent, the only temperature dependences are due to τ and τ_{rad}. In presence of non-radiative processes τ does not coincide with τ_{rad} and I_{PL} depends on temperature. The temperature dependence of the radiative rate ($R_R = 1/\tau_{rad}$) can be extracted by the ratio between the PL intensity and the decay time at fixed photon flux, as shown in Fig. 5(c), where the radiative rate in arbitrary units at each temperature is calculated by dividing the PL intensity by the decay time. R_R increases by about a factor of 200 on going from 11 to 300 K, and this increase is partially counterbalanced by a simultaneous increase in the efficiency of the non-radiative processes as suggested by Fig. 5(b), showing a marked PL lifetime shortening when the temperature is increased. Since it is well known that non-radiative processes are characterized by very fast decay times, we can conclude that these processes have an increased role in the de-excitation dynamics of Si NWs when the temperature is increased.

#157097 - $15.00 USD Received 25 Oct 2011; revised 7 Dec 2011; accepted 7 Dec 2011; published 9 Jan 2012

The behavior of the radiative rate can be explained with a model proposed by Calcott et al. [24] for porous Si and applied also to Si nc [23,25]. According to this model the exchange electron-hole interaction splits the excitonic levels by an energy Δ. The lowest level in this splitting is a triplet state and the upper level is a singlet state. The triplet state (threefold degenerate) has a radiative decay rate R_T much smaller than the radiative decay rate R_S of the singlet. Once excited the excitonic population will be distributed according to thermal equilibrium law. Hence at a temperature T the radiative decay rate will be:

$$R_R = \frac{3R_T + R_S \exp\left(-\frac{\Delta}{kT}\right)}{3 + \exp\left(-\frac{\Delta}{kT}\right)} \qquad (2)$$

Equation (2) suggests that, by increasing temperature, the relative population of the singlet state will increase and, being the radiative rate of the singlet state much higher than that of the triplet state, also the total radiative rate will consequently increase. We have used this formula to fit the data in Fig. 5(c). Indeed the continuous line is a fit to the data with $\Delta = 26.9 \pm 4.3$ meV. This value is in good agreement with those previously found for porous Si [24] and Si nc [23, 25], confirming the occurrence of quantum confinement effects also in Si NWs. Note also that similar values of the level splitting have been recently theoretically calculated for Si NWs [26], though no experimental data existed. Calculations of the splitting of the excitonic levels at detection wavelengths different than 690 nm have been done and the results, showing an increased splitting for lower wavelengths (corresponding to smaller NWs), are in agreement with literature [23, 24].

4. Conclusions

The analysis of the PL properties as a function of aging, temperature and pump power of Si NWs prepared by metal-assisted wet etching strongly supports the idea that photon emission is due to quantum confinement effects. These results open the route towards novel applications of Si NWs in photonics as efficient light sources. Indeed, the synthesis can be also applied over very large area samples, up to the wafer scale, and it is therefore potentially compatible also with the industrial environment typically used for manufacturing Si-based electronic devices. It is also interesting to compare the perspectives in silicon photonics of Si NWs with those of Si nc, which are currently considered the most promising material for the fabrication of Si-based light sources. The data we have reported in this paper show that Si NWs exhibit strong similarities to Si nc from several point of views, and above all with respect to the mechanism of light emission. On the other hand, the strongly reduced influence of Auger non-radiative recombination processes suggests that Si NWs could have an even greater potential for the fabrication of light sources. Furthermore, it is well known that tunneling phenomena are the main conduction mechanism when Si nc embedded in SiO_2 are electrically excited [27]. This determines high operating voltages and oxide breakdown phenomena, which strongly complicate any practical device application of Si nc. All of these drawbacks are absent in Si NWs. Finally, the peculiar high surface reactivity exhibited by the wires, and its influence on the PL properties of the system, makes this material potentially interesting also for sensor fabrication.

Acknowledgments

We wish to thank C. Percolla and S. Tatì for expert technical assistance.

#157097 - $15.00 USD Received 25 Oct 2011; revised 7 Dec 2011; accepted 7 Dec 2011; published 9 Jan 2012